Particle Correlation Observed in e^+e^- Annihilations into Hadrons at c.m. Energies between 29 and 37 GeV

TASSO Collaboration

M. Althoff, W. Braunschweig, F.J. Kirschfink,
H.U. Martyn, R. Rosskamp, H. Siebke[1], W. Wallraff

I. Physikalisches Institut der RWTH Aachen, D-5100 Aachen,
Federal Republic of Germany[11]

J. Eisenmann, H.M. Fischer, H. Hartmann,
A. Jocksch, G. Knop, H. Kolanoski, H. Kück[2],
V. Mertens, R. Wedemeyer

Physikalisches Institut der Universität Bonn, D-5300 Bonn,
Federal Republic of Germany[11]

B. Foster, A. Wood

H.H. Wills Physics Laboratory, University of Bristol,
Bristol BS8 1TL, UK[12]

E. Bernardi, Y. Eisenberg[3], A. Eskreys[4],
R. Fohrmann, K. Gather, H. Hultschig, P. Joos,
B. Klima, U. Kötz, H. Kowalski, A. Lagage,
B. Löhr, D. Lüke, P. Mättig[5], G. Mikenberg[3],
D. Notz, D. Revel[3], D. Trines, T. Tymieniecka[6],
G. Wolf[7], W. Zeuner

Deutsches Elektronen-Synchrotron, DESY, D-2000 Hamburg,
Federal Republic of Germany

E. Hilger, T. Kracht, H.L. Krasemann, E. Lohrmann,
G. Poelz, K.U. Pösnecker

II. Institut für Experimentalphysik der Universität Hamburg,
D-2000 Hamburg, Federal Republic of Germany[11]

D.M. Binnie, P.J. Dornan, D.A. Garbutt, C. Jenkins,
W.G. Jones, J.K. Sedgbeer, D. Su, J. Thomas,
W.A.T. Wan Abdullah[8]

Department of Physics, Imperial College,
London SW7 2AZ, UK[12]

F. Barreiro[9], L. Labarga, E. Ros

Universidad Autonoma de Madrid, Madrid, Spain[15]

M.G. Bowler, P. Bull, R.J. Cashmore, P. Dauncey,
R. Devenish, C.M. Hawkes, G. Heath, D.J. Mellor,
P. Ratoff

Department of Nuclear Physics, Osvord University,
Oxford OX1 3RH, UK[12]

S.L. Lloyd

Department of Physics, Queen Mary College,
London E1 4NS, UK[12]

K.W. Bell, G.E. Forden, J.C. Hart, D.K. Hasell,
D.H. Saxon

Rutherford Appleton Laboratory, Chilton, Didcot,
Oxon OX11 0QX, UK[12]

S. Brandt, M. Dittmar, M. Holder, G. Kreutz,
B. Neumann

Fachbereich Physik der Universität-Gesamthochschule Siegen,
D-5900 Siegen, Federal Republic of Germany[11]

E. Duchovni, U. Karshon, A. Montag, R. Mir,
E. Ronat, G. Yekutieli, A. Shapira

Weizmann Institute, Rehovot 76100, Israel[13]

G. Baranko, A. Caldwell, M. Cherney,
M. Hildebrandt, J.M. Izen, M. Mermikides, S. Ritz,
D. Strom, M. Takashima, H. Venkataramania[10],
E. Wicklund, S.L. Wu, G. Zobernig

Department of Physics, University of Wisconsin,
Madison, WI 53706, USA[14]

1 Now at DEC, Hamburg, FRG
2 Now at Fraunhofer Institut, Duisburg, FRG
3 On leave from Weizmann Institute, Rehovot, Israel
4 On leave from Institute of Nuclear Physics, Cracow, Poland
5 Now at IPP Canada, Carleton University, Ottawa, Canada
6 On leave from Warsaw University, Poland
7 Now at SLAC, Stanford, CA, USA
8 On leave from University of Malaya, Kuala Lumpur
9 Now at University of Siegen, FRG
10 Now at Yale University, New Haven, CT, USA

Abstract. We have studied the correlations between charged particles produced in e^+e^- annihilations into hadrons at c.m. energies between 29 and 37 GeV. We have analysed the correlations between the charged multiplicities of the jets and the two particle rapidity and charge correlations. No evidence for correlations between the multiplicities of the two jets is found. Two particle short range rapidity and charge correlations are observed, indicating that particles cluster in rapidity and that their charges compensate locally. An extensive study of these correlation effects by QCD Monte Carlo calculations was performed. Evidence for charge correlations due to Bose-Einstein statistics is also observed.

1. Introduction

It has been shown that e^+e^- annihilations into hadrons proceeds predominantly through the creation of a $q\bar{q}$ pair and subsequent fragmentation of quarks into hadrons:

$$e^+e^- \to q\bar{q} \to \text{hadrons}.$$

As a consequence, at sufficiently high energy one observes two back to back jets of hadrons. Emission of hard gluons and their subsequent fragmentation results in an observation of a third jet in about (10 −20)% of the events at high energy. These production mechanisms at the parton level, coupled with the fragmentation into hadrons, lead to correlations between the final hadrons which can be studied as a function of different variables characterising the hadrons.

Before entering the detailed discussion of the different types of dynamical correlations, it is worth stressing that conservation of charge, energy and momentum lead to correlation effects in various particle variables. One should also be aware that strong correlations in one variable may simulate or screen correlation effects in others. The following types of correlation will be discussed in this paper:

   i) jet multiplicity correlations;
   ii) rapidity correlations;
   iii) charge correlations in rapidity space;
   iv) correlations induced by the Bose-Einstein statistics.

This paper is an extension of our earlier studies. It is based on much larger statistics than the published results [1, 2].

All four types of correlations have been studied extensively in hadron-hadron collisions [3, 4]. So far the results of similar studies for e^+e^- interactions are scarce.

Since the hadron production process in e^+e^- annihilation is less complicated than in hadron-hadron interactions it is of particular interest to compare results from the latter process with e^+e^- data.

The data used in this analysis were obtained with the TASSO detector during the runs at PETRA in the period of 1981 to 1983. The events were taken with a trigger scheme as described in [5]. For selection of hadronic events the most relevant cuts for this work were on charged particle multiplicity $n_{CH} \geq 5$ and on the momentum sum of all charged particles $\sum |p_i| > 0.265 * W$, W being the c.m. energy.

In order to increase the statistics, events in the c.m. energy interval (29–37) GeV were combined. Most of them however were taken at (34.5–35.5) GeV. In total, 22350 events were selected for the analysis. Our analysis is restricted to charged particles only. No separation according to particle types was made; when necessary a pion mass was assumed.

Except for the multiplicity study the experimental distributions were corrected for acceptance losses and detector biases. They are compared with Monte Carlo distributions, which were generated assuming 5 quark flavours (u, d, s, c, b) and gluon emission (first order in QCD) according to the independent parton fragmentation [6] and string fragmentation schemes [7]. The parameters used in the generation of the MC events were tuned to fit the single particle distributions, as reported in reference [8], in particular, the ratio $PS/(PS+V)$ of pseudoscalar (PS) to pseudoscalar plus vector mesons $(PS+V)$ was taken as 0.5 and the fragmentation functions for c and b quarks were taken from [9] with $\varepsilon = 0.25$ for c and $\varepsilon = 0.04$ for b quark.

For the study of the rapidity and charge correlations the rapidity dependent correction factors for the experimental distributions were obtained with the help of MC events. These correction factors were calculated by dividing the distributions for generated particles by the ones obtained after the generated particles were passed through the detector simulation and all the experimental cuts. The generated particles include all primary fragmentation particles and those produced in the decays of resonances or particles with lifetime shorter than $3 * 10^{-10}$ s.

Except for the Bose-Einstein effect the observed correlations are practically independent of the specific MC model used: the correction factors obtained with the independent jet fragmentation model and the Lund fragmentation model are the same within the errors.

2. Jet Multiplicity Correlations

The correlations discussed in this section are between multiplicities of the charged particles emitted

into two different hemispheres. The hemispheres were defined with respect to the sphericity axis. In most cases, each hemisphere contains a well defined jet. The distinction between the hemispheres is irrelevant for collisions like $e^+ e^-$ and so we shall call arbitrarily one direction forward (backward).

For the analysis presented in this section we used the event sample described in the introduction. The experimental multiplicities were not corrected for acceptance losses.

It is well known that in hadron-hadron interactions at high energies the forward-backward multiplicity correlations are rather strong [10, 11]. If one denotes by $\langle n_F \rangle$ the average multiplicity of the charged particles produced in the forward hemisphere for a given multiplicity n_B of charged particles in the backward hemisphere, then these correlations can be well described by the formula:

$$\langle n_F \rangle = a + b n_B. \tag{2.1}$$

For pp and $p\bar{p}$ interactions, for which the data are most abundant, the parameter b is positive over a

wide energy interval $(20 \lesssim \sqrt{s} \lesssim 540$ GeV) and its value is increasing logarithmically with energy [11]. It was also found that b depends on the rapidity of the considered particles, i.e. b is bigger for particles of small rapidity $(|y| < 1)$ than for particles of large rapidity $(|y| > 1)$ [10, 11]. These observations can be qualitatively explained in the impact parameter picture [12], as the small rapidity particles are produced in the central, large multiplicity collisions while large rapidity particles are produced in the peripheral, small multiplicity collisions. No correlations of this type are expected for $e^+ e^-$ annihilations.

Our experimental dependence of $\langle n_F \rangle$ on n_B is shown in Fig. 1a. Indeed there is at most a weak correlation between these multiplicities in contrast to the situation in pp interactions. The data are reasonably well described by both independent parton fragmentation and string fragmentation MC models. We checked that the slow rise of $\langle n_F \rangle$ with n_B observed in the data is not due to the fact that we merged events at different c.m.s. energies (different average event multiplicities).
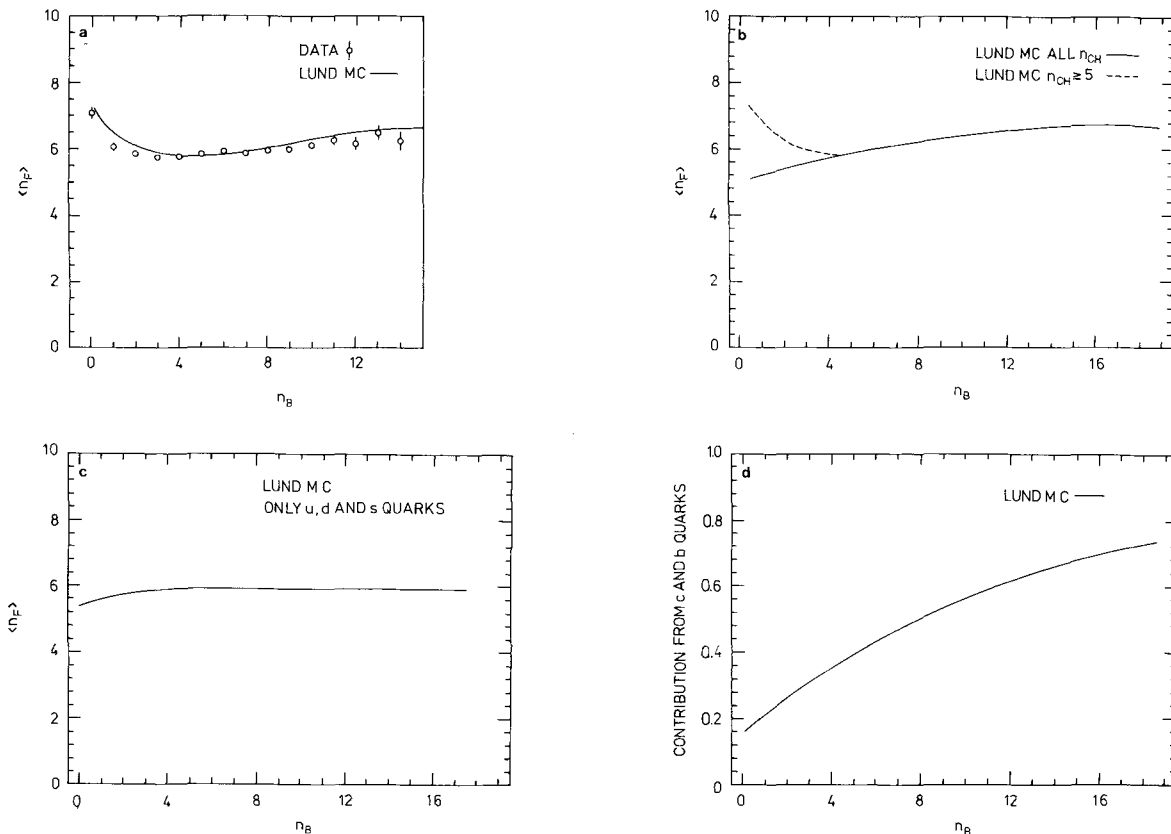

Fig. 1 a–d. Dependence of the average charged multiplicity in one jet $\langle n_F \rangle$ on the charged multiplicity n_B in the other one; **a** for the data uncorrected for the acceptance losses; Lund MC predictions shown by full curve; **b** for full acceptance MC events: all charged multiplicities (full curve) and for charged multiplicities $n_{CH} \geq 5$ (dashed curve); **c** for full acceptance MC events generated with u, d and s quarks; **d** fraction of c and b quark events as a function of charged multiplicity in the jet n_B
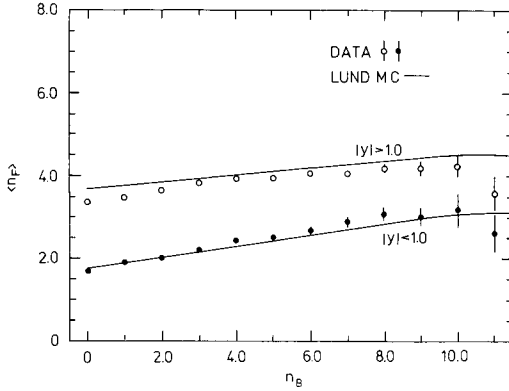
Fig. 2. Same as Fig. 1a but for two intervals of particle rapidities: $|y| < 1$ and $|y| > 1$

Since the agreement between the data and the MC calculation is good, one can attempt to understand the observed weak correlations between $\langle n_F \rangle$ and n_B by studying MC generated events. In Figs. 1b, c and d we show curves obtained for MC events, generated with full acceptance (i.e. not passed through the detector simulation and experimental cuts). The increase of $\langle n_F \rangle$ with decreasing n_B for small n_B values can be understood from Fig. 1b. In this figure two MC curves are shown, one for events with $n_{CH} \geq 5$ (dashed curve) and the other for all events (full curve). The experimentally observed rise at low n_B is generated by the multiplicity cut $n_{CH} \geq 5$. The slow rise of $\langle n_F \rangle$ with n_B for larger n_B values is due to the contribution of heavy quarks (defined as the ratio of the number of heavy quark events to all generated events), which is increasing with n_B – Fig. 1d. Indeed, if one removes heavy flavours (c and b), the fragmentation of which leads on average to larger multiplicities, no correlation is observed – see Fig. 1c.

In analogy to similar studies made for pp collisions we show in Fig. 2 the experimental dependence of $\langle n_F \rangle$ on n_B for the two rapidity intervals: $|y| < 1$ and $|y| > 1$. Rapidity is defined with respect to the sphericity axis. A slow rise of $\langle n_F \rangle$ with increasing n_B is observed for both rapidity intervals. The general trend of the data is reproduced by the Lund fragmentation MC.

In conclusion, we observe a very weak correlation between multiplicities in opposite jets. This is reproduced by the Lund MC. The weak correlation observed is partly generated by our experimental multiplicity cut and is partly due to the contribution from the fragmentation of heavy quarks. This is in contrast with the situation for hadron-hadron interactions.

3. Rapidity Correlations

In this section we discuss the correlations between the two particles of type a and b with rapidities y_1 and y_2 respectively. In order to study these correlations quantitatively one defines the function [3]:

$$C^{a,b}(y_1, y_2) = \rho_2^{a,b}(y_1, y_2) - f \rho_1^a(y_1) \rho_1^b(y_2) \qquad (3.1)$$

where $\rho_2^{a,b}(y_1, y_2) = (1/\sigma) \, (d^2\sigma/(dy_1, dy_2))$ is the two particle density and $\rho_1 = (1/\sigma) \, (d\sigma/dy)$ is the one particle density.

σ is the total cross section and f is a normalisation factor. If one requires that in the absence of correlation $C^{a,b}(y_1, y_2) = 0$ then

$$f = \langle n_a(n_b - \delta^{a,b}) \rangle / \langle n_a \rangle \langle n_b \rangle \qquad (3.2)$$

where n_a and n_b are the multiplicities of particle types a and b respectively, $\delta^{a,b} = 0$ when one distinguishes particle types a and b and $\delta^{a,b} = 1$ if one does not. In the literature the normalised correlation function $R(y_1, y_2)$ is used more frequently:

$$
\begin{aligned}
R(y_1, y_2) &= \frac{C^{a,b}(y_1, y_2)}{f \rho_1^a(y_1) \rho_1^b(y_2)} \\
&= \frac{\rho_2^{a,b}(y_1, y_2)}{f \rho_1^a(y_1) \rho_1^b(y_2)} - 1.
\end{aligned} \qquad (3.3)
$$

This normalised correlation function is expected to be less sensitive to acceptance corrections and less dependent on particle multiplicity.

Since both correlation functions (3.1) and (3.3) are functions of two variables one fixes the value or interval of one variable ("trigger") and examines the dependence on the other one. We chose four intervals for the trigger rapidity: $(-5.5, -2.5)$, $(-2.5, -1.5)$, $(-1.5, -0.75)$ and $(-0.75, 0)$, maximum (pion) rapidity being 5.6 at the highest energy. Since the rapidity distribution is symmetric around $y = 0$, the correlation functions for positive and negative trigger rapidities were added.

The experimental sample used in the analysis of these correlations was the sample described in the introduction.

In Figs. 3a–d we show the corrected normalised correlation functions $R(y, y_t)$ for the four intervals of the trigger particle rapidity y_t. In all four intervals maxima are observed for $y \approx y_t$ and except for the highest y_t the correlation functions are positive at the maximum. This is a demonstration of short range correlations ($|y - y_t| \lesssim 1$), especially for small trigger rapidities (see Fig. 3d).

Since it was shown that the mere mixing of events of different multiplicities may lead to substantial correlation effects [13], we checked that the
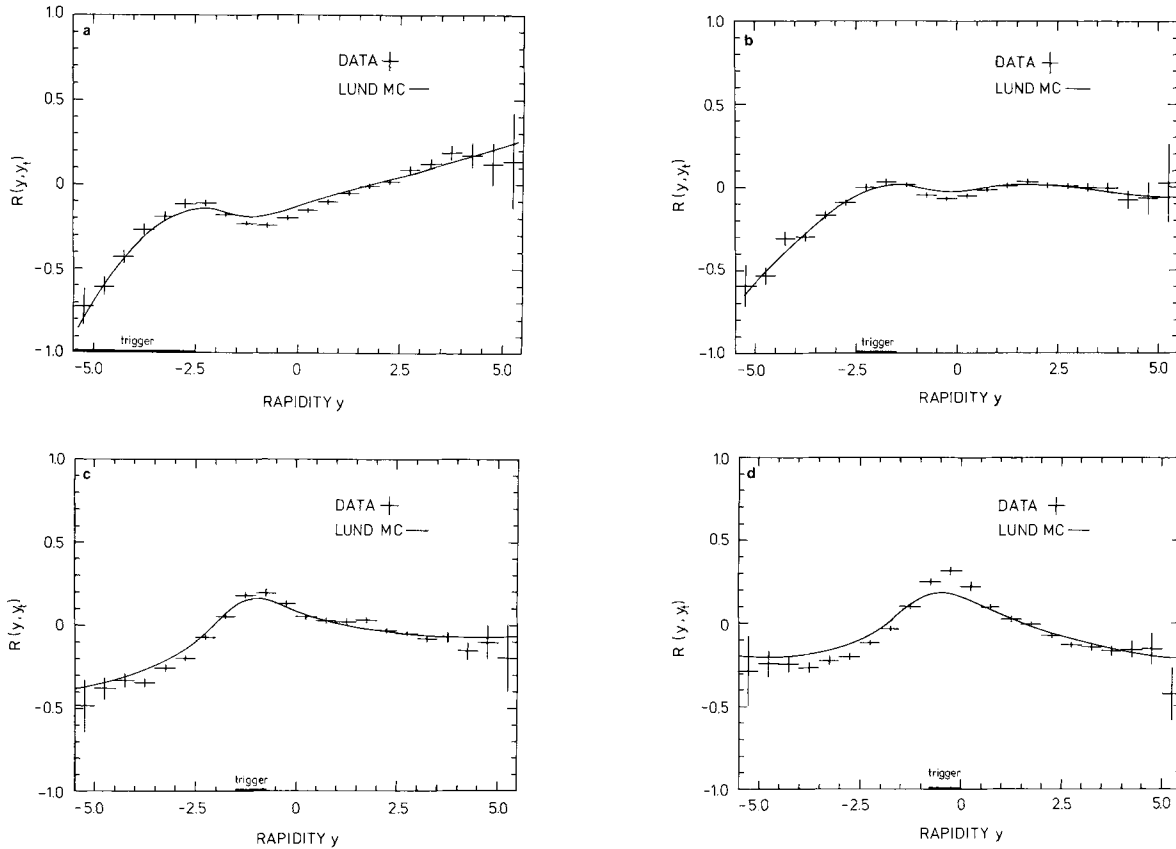
Fig. 3a–d. Rapidity correlation functions $R(y, y_t)$ for four trigger rapidity y_t intervals: **a** $(-5.5, -2.5)$, **b** $(-2.5, -1.5)$, **c** $(-1.5, -0.75)$, and **d** $(-0.75, 0)$. Data are corrected for acceptance losses. Lund MC predictions are shown by full curves

short range correlation maximum is also visible and significant for reactions of fixed charged multiplicity. One can see this in Fig. 4, where we show the uncorrected correlation functions $R(y, y_t)$ for $-0.75 < y_t < 0$ and charged multiplicities $n_{CH} = 6, 12$
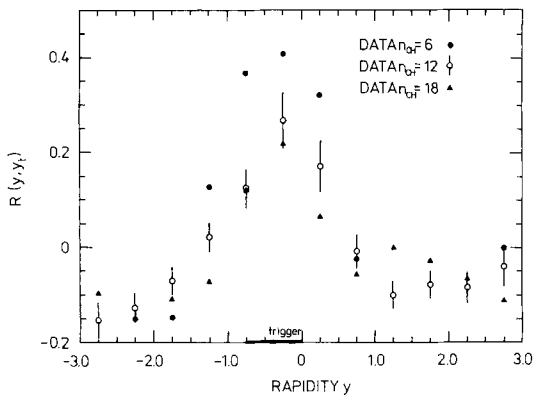

Fig. 4. Experimental rapidity correlation function $R(y, y_t)$ for trigger rapidities $-0.75 < y_t < 0$ and charged multiplicities $n_{CH} = 6, 12$ and 18. Data are not corrected for acceptance losses

and 18. An indication for a multiplicity dependence is also observed – the height of the maximum increases with decreasing multiplicity.

The curves drawn in Figs. 3a–d are for the Lund MC events. Their agreement with the experimental points is good if one keeps in mind that the MC parameters were tuned using only single particle distributions. A similar type of correlations was observed for hadron-hadron collisions [3] and was successfully reproduced by cluster models [14]. These clusters were interpreted as being predominantly resonances. Since the selection of resonances is experimentally impossible and the agreement between the data and MC shown in Figs. 3a–d is good, one can check the effects of resonances using the MC generated events (with full acceptance). In Figs. 5a–d we show the comparison of the function $R(y, y_t)$ calculated for primary fragmentation particles i.e. before the resonances decayed (full curve) with that for all generated particles i.e. after the resonances decayed (dashed curve). Except for the smallest trigger rapidities (Fig. 5d) the influence of the resonance production is visible. For the highest
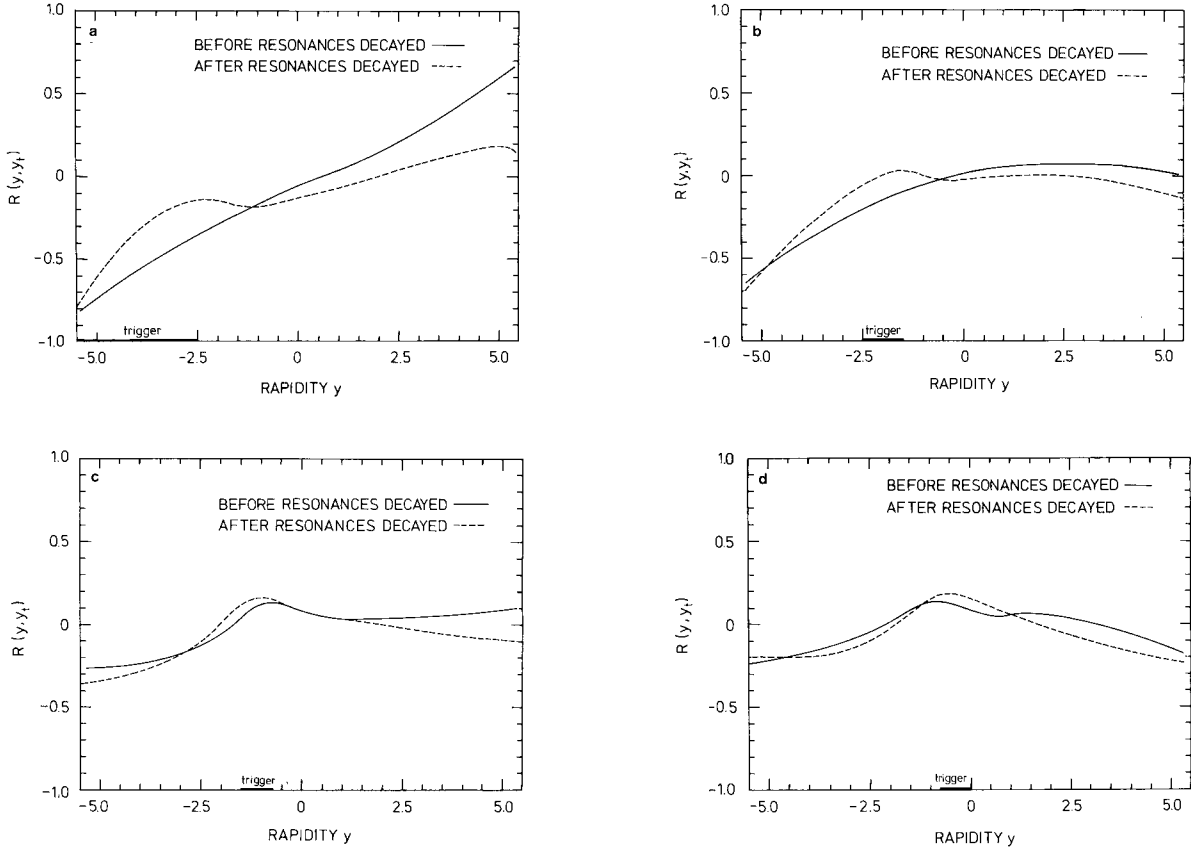
Fig. 5a–d. Rapidity correlation functions $R(y, y_t)$ for full acceptance Lund MC events and for four trigger rapidity intervals: **a** $(-5.5, -2.5)$, **b** $(-2.5, -1.5)$, **c** $(-1.5, -0.75)$, and **d** $(-0.75, 0)$. Curves shown in the figures correspond to primary fragmentation particles (full) and to all fragmentation particles (dashed)

rapidities the short range correlation maximum is mostly due to the resonances, while at small rapidities their role is small.

A direct comparison of our results with those obtained for hadron-hadron collisions is difficult. In hadron-hadron interactions the bulk of lower multiplicity events comes from the diffraction dissociation processes, which are of a very specific nature and do not have any analogue in e^+e^- annihilations. Thus before any comparison can be made, these events have to be removed from the hadron-hadron sample. The simplest way is to require that the charged multiplicity is large (e.g. $n_{CH} \geq 8$). One should also make sure that the energies and multiplicity cuts in the samples to be compared are not too different (although both the energy and multiplicity dependence of the rapidity correlations were found to be rather weak [3]). The ABCHW Collaboration [15] published $pp/\bar{p}p$ correlation data at $\sqrt{s} = 53$ GeV and $n_{CH} \geq 8$. In Fig. 6 we compare our results ($\sqrt{s} = 34$ GeV, $n_{CH} \geq 5$) with those of the ABCHW Collaboration. It is seen that the maximum due to the

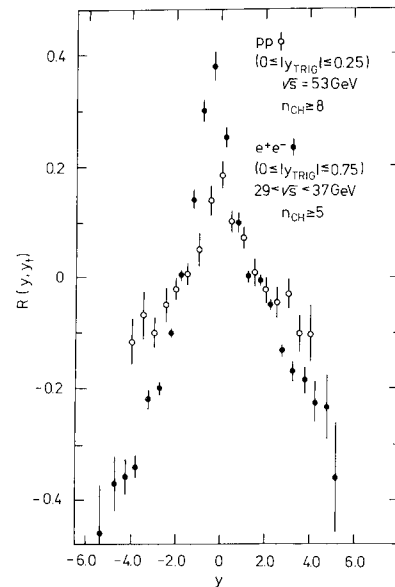**Fig. 6.** Comparison of the rapidity correlation function $R(y, y_t)$ from this experiment with that from the pp experiment of the ABCHW Collaboration [15]
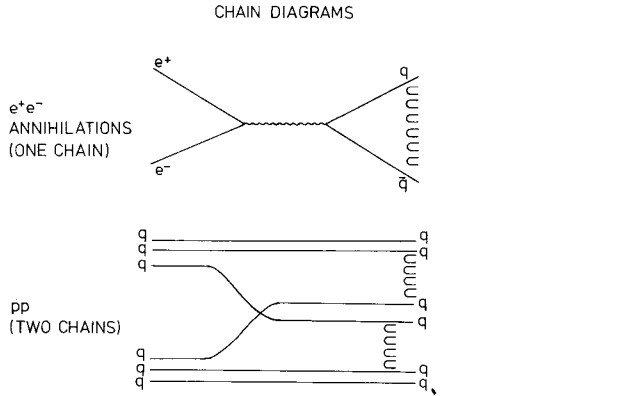
CHAIN DIAGRAMS

e^+e^-
ANNIHILATIONS
(ONE CHAIN)

pp
(TWO CHAINS)

Fig. 7. Chain diagrams for $e^+ e^-$ annihilations and pp interactions

short range correlations is higher for $e^+ e^-$ annihilations than that for pp collisions. These observations can be interpreted within the frame of the multichain dual model [16]. In this model the production of particles occurs through the breaking of the color chains stretched between quark and antiquark ($e^+ e^-$ annihilations) or between quark and

diquark (pp collision) – Fig. 7. Thus in the lowest order, one deals with one chain in $e^+ e^-$ annihilations, while in pp collisions two chains are effective. For the two chain case, under the assumption that the chains are uncorrelated, one expects the correlation function [2]:

$$R_{pp} = \frac{R^{(1)} \rho^{(1)}(y) \rho^{(1)}(y_t) + R^{(2)} \rho^{(2)}(y) \rho^{(2)}(y_t)}{(\rho^{(1)}(y) + \rho^{(2)}(y_t))(\rho^{(1)}(y_t) + \rho^{(2)}(y))} \qquad (3.4)$$

as expressed in terms of one chain correlation functions $R^{(1)}$ and $R^{(2)}$ and one chain density functions $\rho^{(1)}$ and $\rho^{(2)}$. Assuming chain universality: $R^{(1)} \approx R^{(2)} \approx R_{ee}$ and $\rho^{(1)} \approx \rho^{(2)}$ one gets

$$R_{pp}(y, y_t) \approx 1/2 R_{ee}(y, y_t) \qquad (3.5)$$

in qualitative agreement with Fig. 6.

In summary, we observe genuine dynamical two particle rapidity correlations of the range of one unit in rapidity, for all studied rapidity regions. A significant contribution to these correlations, especially for large trigger rapidities comes from the production and decay of resonances, although in addition the
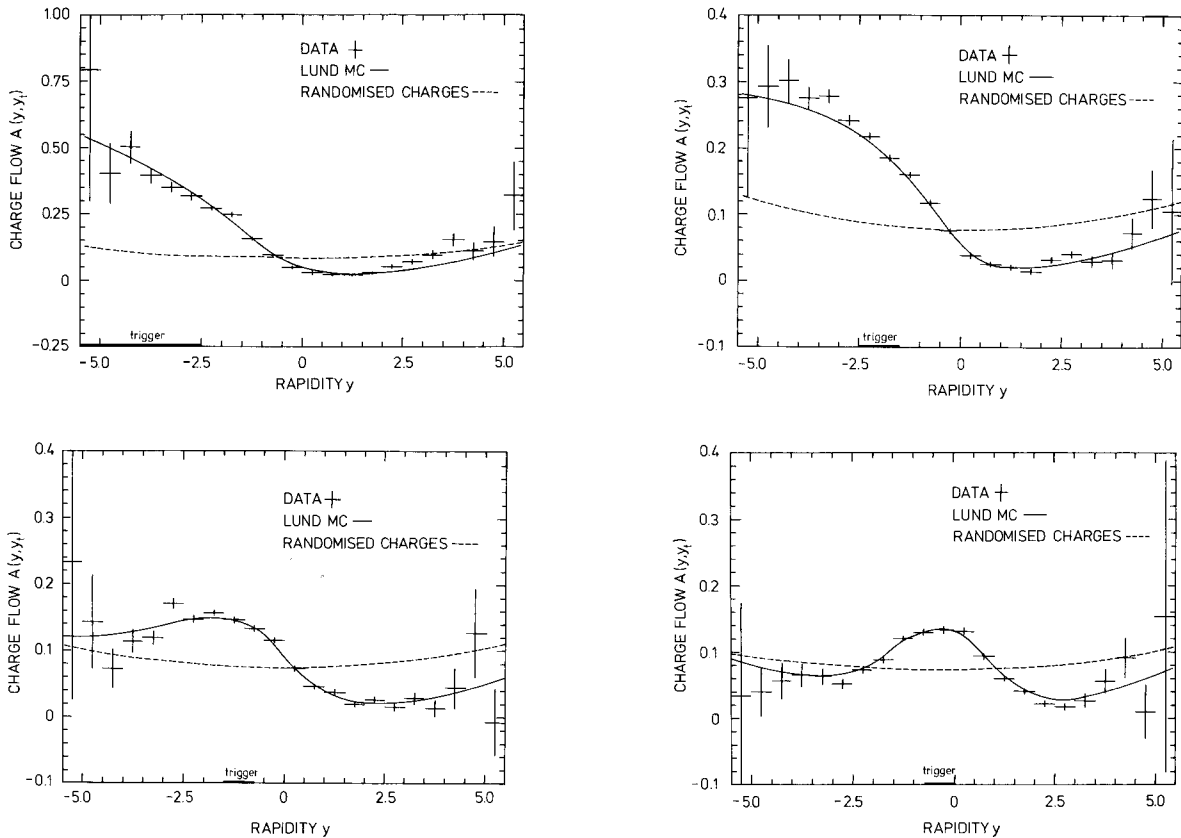

Fig. 8a–d. Compensating charge flow functions $A(y, y_t)$ for four trigger rapidity y_t intervals: **a** $(-5.5, -2.5)$, **b** $(-2.5, -1.5)$, **c** $(-1.5, -0.75)$, and **d** $(-0.75, 0)$. Data are corrected for acceptance losses. Lund MC predictions are shown with full curves. Dashed curves are for events with randomised particle charges

fragmentation process alone has a sizable contribution. A comparison with pp data indicates a similar pattern of correlation functions.

4. Two Particle Charge Correlations

Correlations between charges of two particles with rapidities y and y_t have been studied for e^+e^- annihilations by the TASSO [1], PLUTO [17] and TPC [18] Collaborations. Here we present an extended analysis based on much larger statistics than in [1].

Following our previous approach [1], we define the charge correlation function:

$$\Psi_r(y, y_t) = (\bar{\rho}_2^{+-}(y, y_t) + \bar{\rho}_2^{-+}(y, y_t))$$
$$- (\bar{\rho}_2^{++}(y, y_t) + \bar{\rho}_2^{--}(y, y_t)) \qquad (4.1)$$

where

$$\bar{\rho}_2(y, y_t) = \sum (1/n)\, \rho_{2,n}(y, y_t)$$

n is the event charged multiplicity and $\rho_{2,n}$ is the two particle density defined in Sect. 3, for a given charged multiplicity $n_{CH} = n$. The superscripts refer to the particle charges. Thus $\bar{\rho}_2$ is the two particle density renormalised in such a way that each event contributes with the same weight and for a particle at $y = y_t$ with a given charge, Ψ_r is proportional to the difference in the probabilities that another particle at y will have like $(\bar{\rho}_2^{++}, \bar{\rho}_2^{--})$ or unlike $(\bar{\rho}_2^{-+}, \bar{\rho}_2^{+-})$ charge.

Since Ψ_r describes a convolution of both the rapidity and charge correlations, it is useful to introduce also a quantity for which the influence of the rapidity correlations is suppressed. This quantity, called the compensating charge flow [1], is defined as follows:

$$A(y, y_t) = \Psi_r(y, y_t)/(\bar{\rho}_2^{+-}(y, y_t) + \bar{\rho}_2^{-+}(y, y_t)$$
$$+ \bar{\rho}_2^{++}(y, y_t) + \bar{\rho}_2^{--}(y, y_t)). \qquad (4.2)$$

The sample of events used in this analysis is the same as the one described in the introduction with an additional cut requiring that the observed net charge of each event is $|\sum Q_i| \leq 2$. This reduces our sample to 18570 events. The experimental distributions were corrected for the acceptance losses and detector biases as previously discussed.
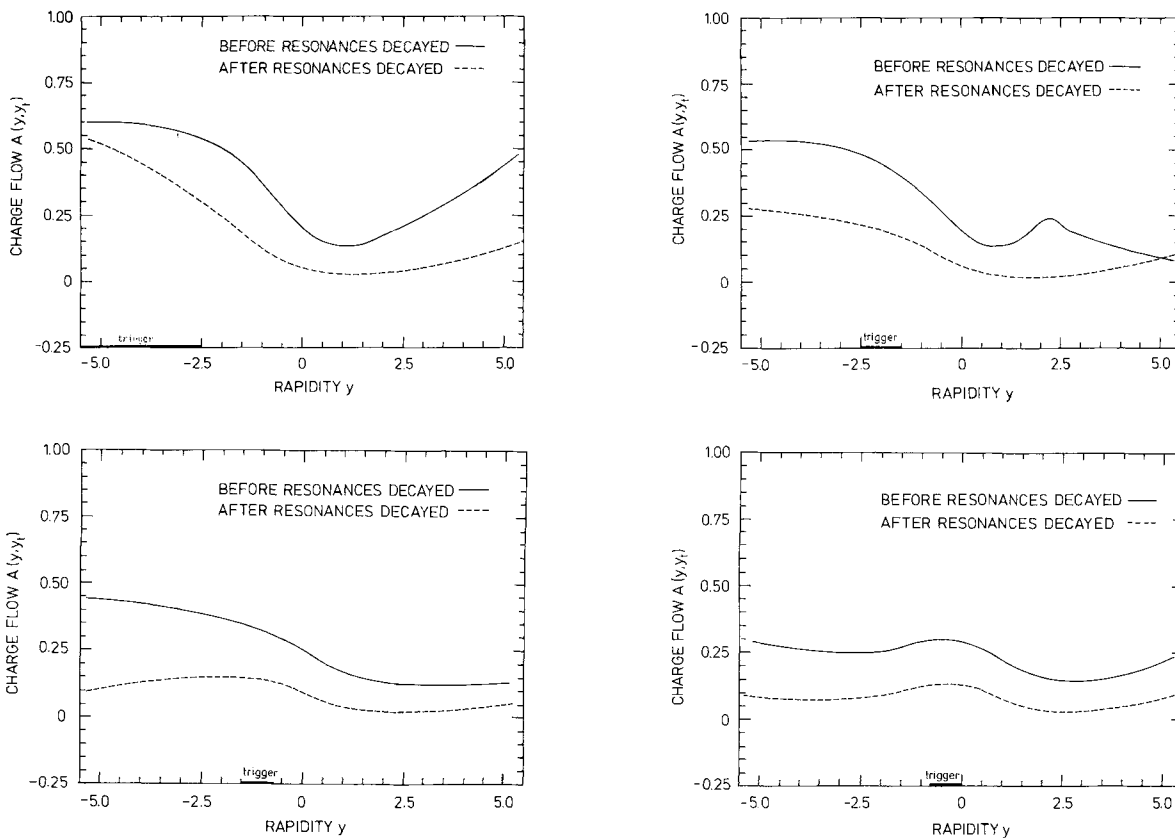

Fig. 9a–d. Compensating charge flow functions $A(y, y_t)$ for MC events generated with full acceptance, for four trigger rapidity y_t intervals: a $(-5.5, -2.5)$, b $(-2.5, -1.5)$, c $(-1.5, -0.75)$, and d $(-0.75, 0)$

In Figs. 8a–d we show the compensating charge flow functions $A(y, y_t)$. In these figures short range effects are observed: for small values of the difference $|y - y_t| < 1$ maxima or shoulders are observed indicating that the particle charges tend to compensate locally in rapidity.

Figures 8a–b are relevant for the problem of long range charge correlations. For large values of y there is an agreement between the data and the Lund MC calculations (full curves), which have long range correlation via primary charged partons built in.

In the same figures we show the distributions obtained from the data when charges of the particles are randomised within each event, leaving the total net charge in the event unchanged (dashed curves). In this case, the genuine dynamical charge correlations should be suppressed, while leaving unaffected the reflections of the rapidity correlations and charge conservation. These distributions are almost flat in rapidity while the data show a clear structure.

Again, it is interesting to see what are the effects of resonance decays. We proceed in a way analogous to that described in the previous section, by using the MC generated events. The compensating charge flow functions shown in Figs. 9a–d refer to primary fragmentation particles (full curves) and to all generated particles i.e. including resonance decay products (dashed curves). Here the resonance production and decay decreases the value of $A(y, y_t)$, and tends to smear out the structure present for primary fragmentation particles. Therefore a large fraction of the short range charge correlations can be explained by a short range order in the fragmentation process.

5. Bose-Einstein Correlations

This type of correlation is induced by the Bose-Einstein symmetry of the wave functions of identical bosons (GGLP effect [19]), which leads to clustering in phase space of identical bosons. The traditional way to investigate these correlations is to look at the ratio of the number of identical to non-identical pion pairs, as a function of their effective mass, or of the difference of their momenta. This ratio shows an enhancement for small values of the effective mass, or momentum difference. The maximum possible enhancement is a factor of 2 for pion pairs and 6 for pion triplets. It was shown [20–22], that the size and shape of this enhancement is correlated with the spatial and temporal extension of the pion source and the degree of coherence in pion emission. Several parametrisations of this enhancement, in terms of the variables constructed from the particle momenta

were proposed [4, 21, 23]. Here we adopt the parametrisation proposed in [23]. The ratio R_{BE} of identical to non-identical pion pairs, or triplets is given by:

$$R_{BE}(Q^2) = 1 + \alpha e^{-\beta Q^2} \qquad (5.1)$$

where $Q^2 = M_{EFF}^2 - 4 \cdot m_\pi^2$ for pion pairs and $Q^2 = M_{EFF}^2 - 9 \cdot m_\pi^2$ for pion triplets and M_{EFF} is the effective mass of the system. This parametrisation can be obtained from the Fourier transform of a spherical pion source of Gaussian density as observed from the pion pair or pion triplet rest frame. In this reference frame the four momentum difference is: $|\tilde{p}_1 - \tilde{p}_2|^2 = |\vec{k}_1 - \vec{k}_2|^2 = Q^2$ where $\tilde{p}$ and $\vec{k}$ are the four and three momentum vectors of particles in a pair. It was argued [23, 24], that the parameter β can be treated as a measure of the pion source extension, as seen from the pion pair rest system, while the parameter α measures the strength of the effect and thus the degree of coherence in the pion emission. For completely coherent emission $\alpha = 0$.

We present in this section the results for the pion pairs and triplets, using the parametrisation (5.1), leaving the detailed discussion of this parametrisation and the interpretation of the data to further investigation.

For the sample of events used in this analysis an additional track cut was introduced. The distance d_0 by which a track misses the interaction vertex was required to be smaller than 0.5 cm, to reduce the number of pions from K^0 and Λ^0 decays and electrons from γ conversions. No attempt was made to remove pions from decay of such resonances as ρ^0 which are so short lived that they can be regarded as part of the pion source (in any case identification of their contribution is impossible). All charged particles were taken to be pions.

The effective mass spectra for the unlike and like pion pairs are shown in Figs. 10a–b. In Fig. 10a a maximum at the position of the K^0 is still visible as well as a shoulder at the position of the ρ^0. The maximum at the K^0 position shows that the suppression of K^0 decay products was incomplete.

In Fig. 11a we show the experimental ratio R_{BE} of the number of like charge $(+ +, - -)$ pion pairs to the number of unlike charge $(+ -)$ as a function of Q^2, uncorrected for acceptance losses. The corresponding ratio for the three pion system is shown in Fig. 11b. In this case, the like charge combinations are $(+ + +)$ and $(- - -)$ and the unlike ones: $(+ + -)$ and $(+ - -)$. In the absence of Bose-Einstein and charge correlations and resonance production these ratios should be constant over the whole range of Q^2 and equal to the ratio of the total
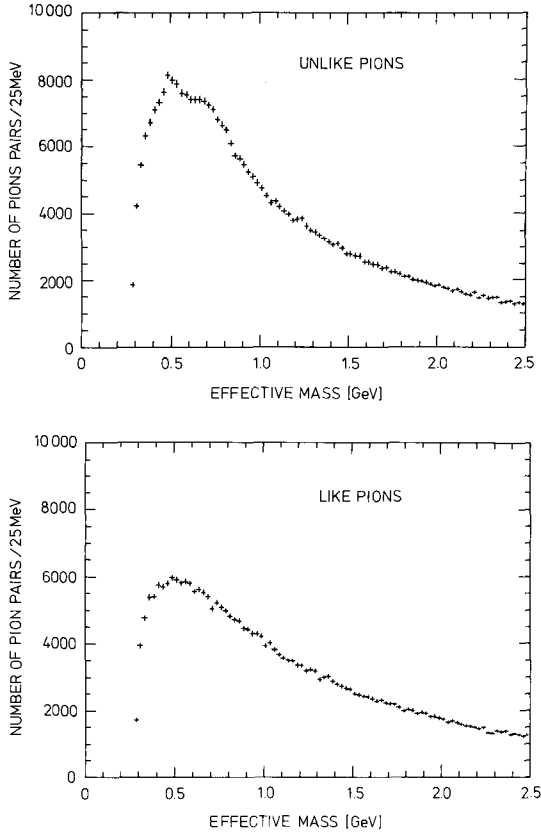
Fig. 10a and b. Effective mass distributions for pion pairs: **a** unlike pions, **b** like pions
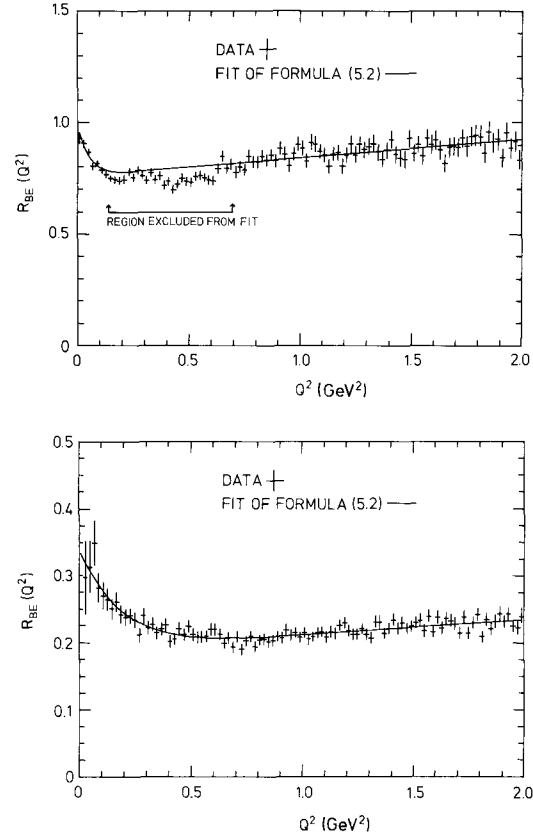

Fig. 11a and b. Ratio R_{BE} of the number of like pion combinations to the unlike ones as function of Q^2, for the uncorrected data: **a** pion pairs, **b** pion triplets

number of like pion combinations to that of unlike ones, in the whole sample. Both distributions display a statistically significant increase of R_{BE} for $Q^2 \to 0$. The value of R_{BE} for two pion systems shows in addition minima at the positions of the K^0 and the ρ^0 resonances.

In order to determine the significance of the rise of R_{BE} for small Q^2 we have fitted distributions in Figs. 11a and 11b (excluding the K^0 and ρ^0 regions for the two pion case) to the formula:

$$R_{BE}(Q^2) = \gamma(1 + \delta Q^2)(1 + \alpha e^{-\beta Q^2}) \qquad (5.2)$$

where α, β, γ and δ are the parameters of the fit and

α – measures the strength of the effect,
β – is a measure of the radius squared of the source,
γ – is an overall normalisation factor and
δ – describes the slow rise of R_{BE} with Q^2.

The fits yield the values of α and β listed in Table 1. In absence of the GGLP effect α should equal 0, while in both cases it is significantly different from 0. This convinces us that the raw data show a GGLP effect.

There are several reasons to expect that the true effect is stronger than that seen in the uncorrected data. First, there are detection inefficiencies. They will reduce the effect if low Q^2 like sign pairs are reconstructed less efficiently than the corresponding unlike pairs, due to the overlap in the tracking chambers. Secondly, among the tracks accepted for the analysis there are still unidentified electrons, kaons and baryons. Electrons from γ conversion will contribute to unlike pairs at very small values of Q^2. Thirdly, the incomplete suppression of the K^0 and Λ^0 decays leaves pions which come from these decays.

Monte Carlo studies indicate that the last two effects leave at small Q^2 values (<0.5 GeV^2) $\sim 30\%$ of particle pairs and $\sim 40\%$ of triplets, containing a non-pion or a pion from a K^0 or Λ^0 decay. These pairs do not show Bose-Einstein correlations.

Finally, local charge compensation and relatively long lived resonance production are also mechanisms which would reduce the value of the parameter α.

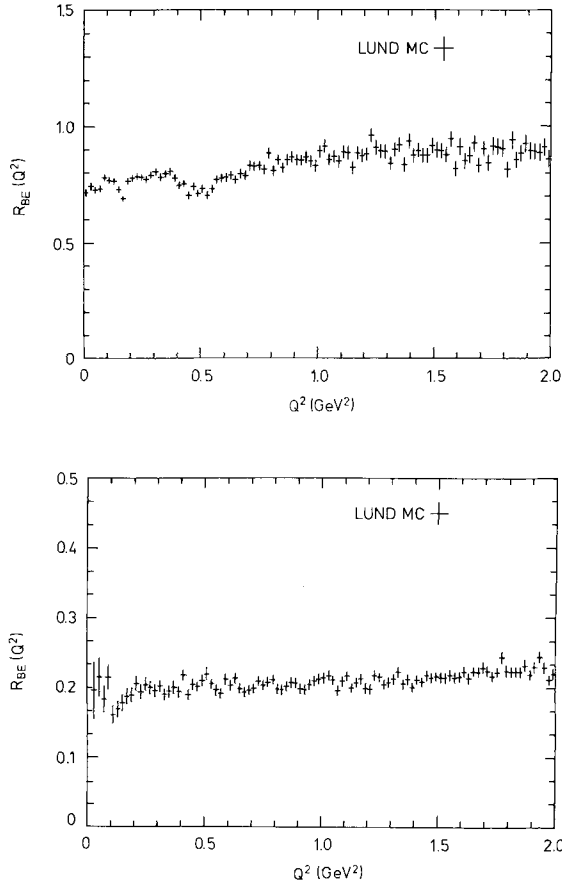In order to check the influence of the above

Fig. 12a and b. Ratio R_{BE} of the number of like pion combinations to the unlike ones as function of Q^2, for MC events with detector simulation and experimental cuts: **a** pion pairs, **b** pion triplets

Fig. 13a and b. Uncorrected experimental ratio R_{BE} (DATA) normalised by the corresponding MC ratio R_{BE} (MC): **a** for pion pairs, **b** pion triplets

effects on the R_{BE} ratio we have used the MC events, which have been generated according to the independent parton fragmentation and Lund fragmentation models without Bose-Einstein symmetrisation and which were passed through the detector simulation and the experimental cuts. The corresponding MC distributions for the Lund fragmentation model are shown in Figs. 12a and 12b. Neither of the distributions shows a rise towards $Q^2 \to 0$.

Since our MC events do not contain Bose-Einstein correlations, but contain many of the effects which suppress these correlations we correct the experimental ratio R_{BE} by dividing it by the corresponding MC ratio. These corrected distributions (with Lund M.C.) are shown in Figs. 13a and 13b. They are smoother than the uncorrected ones; the rise at low Q^2 is stronger; the minima associated with resonances have almost vanished and beyond the small Q^2 region the ratio is roughly constant and consistent with 1. One can obtain satisfactory fits to these distributions with formula (5.2). For the
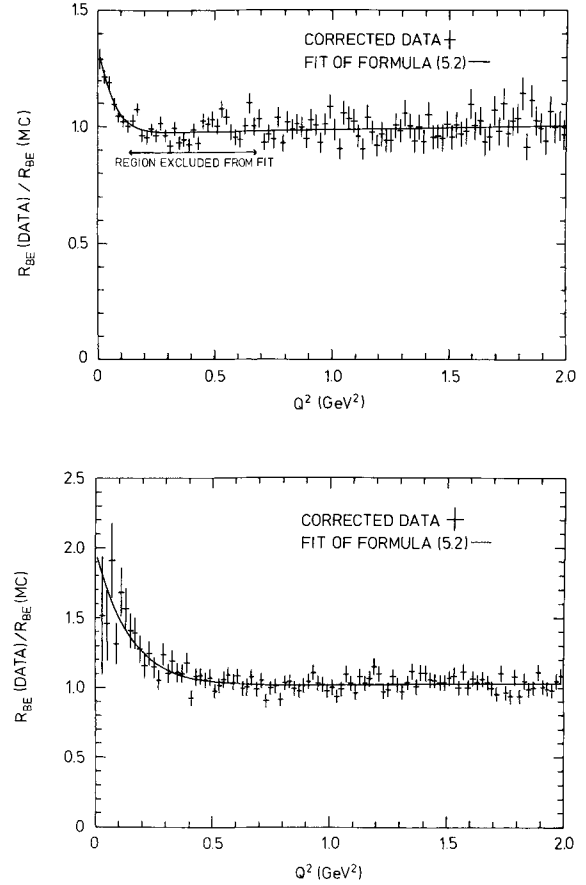
two pion case the fits were performed both including and excluding the K^0 and ρ^0 regions: 0.14 GeV$^2 < Q^2 < 0.7$ GeV^2. The results of these fits are summarised in Table 1 and shown by full curves in Figs. 13a and b. In Table 1 both the statistical and systematic errors are quoted. The main sources of the systematic errors are: imperfect suppression of gamma conversions and of K^0 and Λ^0 decays, limited effective mass resolution (~ 25 MeV) and imperfect match between the MC and data outside the small Q^2 region. The systematic errors were estimated by:

i) varying the fit conditions (changing the Q^2 regions and the resonance cuts, changing the number of parameters);

ii) relaxing the cuts to suppress gamma conversions and K^0 and Λ^0 decays;

iii) changing the binning of the distributions;

iv) using different fragmentation schemes for the correction of the experimental distributions [6, 7].

As can be seen from Table 1 the value of param-

Table 1. Results of the fit of formula (5.2) to the experimental distributions in the Q^2 region (0–2) GeV^2. For ratios marked with *, the Q^2 region (0.14–0.7) GeV^2 was excluded. Systematic errors (in brackets) are quoted only for corrected ratios. Two MC models were used for correction: LM-Lund fragmentation model and IPM-independent parton fragmentation model

Ratio	α	β (GeV^{-2})	r (fm)
$R^{2\pi}_{BE}(Q^2)$*	0.31 ± 0.04	20.0 ± 4.2	0.88 ± 0.09
$R^{2\pi}_{BE}(DATA)/R^{2\pi}_{BE}(IPM)$	$0.57\pm0.04\pm(0.05)$	$15.3\pm1.5\pm(3.0)$	0.77 ± 0.14
$R^{2\pi}_{BE}(DATA)/R^{2\pi}_{BE}(LM)$	$0.42\pm0.04\pm(0.05)$	$16.3\pm2.3\pm(3.0)$	0.77 ± 0.10
$R^{2\pi}_{BE}(DATA)/R^{2\pi}_{BE}(IPM)$*	$0.58\pm0.05\pm(0.05)$	$15.4\pm1.9\pm(3.0)$	0.77 ± 0.15
$R^{2\pi}_{BE}(DATA)/R^{2\pi}_{BE}(LM)$*	$0.45\pm0.05\pm(0.05)$	$15.3\pm2.7\pm(3.0)$	0.76 ± 0.12
$R^{2\pi}_{BE}(Q^2)$	0.85 ± 0.10	5.3 ± 0.8	0.45 ± 0.04
$R^{3\pi}_{BE}(DATA)/R^{3\pi}_{BE}(IPM)$	$1.31\pm0.15\pm(0.10)$	$6.0\pm0.7\pm(1.5)$	0.48 ± 0.11
$R^{3\pi}_{BE}(DATA)/R^{3\pi}_{BE}(LM)$	$0.99\pm0.19\pm(0.10)$	$6.9\pm1.3\pm(1.5)$	0.52 ± 0.07

Table 2. Comparison with other e^+e^- experiments

Experiment	Reaction	$\sqrt{s}$ (GeV)	Pion system	α	r (fm)
MARK II [23]	$J/\Psi \to$ hadrons	3.1	2π	0.71 ± 0.03	0.85 ± 0.02
	$J/\Psi \to 3\pi^+ 3\pi^- + X$	3.1	3π	2.33 ± 0.06	0.49 ± 0.01
	$e^+e^- \to$ hadrons	4–7	2π	0.52 ± 0.06	0.77 ± 0.08
	$e^+e^- \to 3\pi^+ 3\pi^- + X$	4–7	3π	1.09 ± 0.11	0.39 ± 0.04
TPC [24]	$e^+e^- \to$ hadrons	29	2π	0.61 ± 0.08	0.65 ± 0.06
This experiment[a]	$e^+e^- \to$ hadrons	29–37	2π	0.60 ± 0.09	0.76 ± 0.12
	$e^+e^- \to$ hadrons	29–37	3π	1.65 ± 0.36	0.52 ± 0.07

[a] Values of α were corrected for non-pion contamination, correcting factors being 1/0.70 for pion pairs and 1/0.60 for pion triplets. For three pions the values of α were not corrected for two pion correlations.

eter α dependes on the MC used for the correction. For further study we have used the Lund fragmentation model. The systematic errors quoted in this table account only for the effects i) to iii). In order to determine the true strength (α) of the correlations for the three pion system one has to account for the fact, that in the dominator of $R^{3\pi}_{BE}$ we have in this case ($+ + -$) and ($- - +$) combinations, which contain already the correlations of the two pion strength. To correct, one has to multiply $R^{3\pi}_{BE}(Q^2=0)$ by $(1+\alpha^{2\pi})$ and thus $R^{3\pi}_{BE}(Q^2=0) \sim 2.84$. Both $R^{2\pi}_{BE}(Q^2=0)$ and $R^{3\pi}_{BE}(Q^2=0)$ are much below their maximal possible values (2 and 6 respectively).

One has to remember however, that even the corrected ratio: $R_{BE}(DATA)/R_{BE}(MC)$ still contains background coming from non-pions or pions coming from K^0 and Λ^0 decays. This background would tend to suppress the correlation effect. A Monte Carlo calculation shows, that at the value of d_0 cut at 0.5 cm chosen, it will lower the value of α by 30–40%. The influence of this background on β is small. Values obtained by us after correcting for this

background, are in good agreement with those obtained by other e^+e^- experiments [23, 24] – see Table 2. No correction for pions from decays of other long lived particles, in particular D's, B's and η was made. Such a correction would increase our value of α given in Table 2.

It is interesting to check these correlations for various event and pion pair selections. We have investigated the dependence of the observed correlation effect for pion pairs on the event sphericity, the event charged multiplicity, the pion momentum difference in a pair and the pion pair Lorentz factor. The selections applied are listed in Table 3, together with the values of parameters α and β obtained by fitting the corrected ratio $R_{BE}(DATA)/R_{BE}(MC)$ for the selected samples. Within quoted errors none of the selections leads to a significant change in the values of the fit parameters.

There have been suggestions [23, 24], that β measures directly the spatial extension of the pion source as seen from the pion pair rest frame and that α measures the coherence of the pion emission.

Table 3. Results of the fit of formula (5.2) for various selections (in all fits the Q^2 region (0.14–0.7) GeV^2 is excluded). Δp = pion momentum difference

Selection	α	β (GeV^{-2})
Sphericity < 0.1	0.31 ± 0.06	13.1 ± 3.1
$\Delta p < 0.1$ GeV	0.53 ± 0.09	13.6 ± 4.1
$n_{CH} < 12$	0.49 ± 0.08	16.5 ± 3.7
$n_{CH} > 12$	0.44 ± 0.06	16.7 ± 3.0
$\gamma_L < 4$	0.47 ± 0.07	15.8 ± 2.8
$\gamma_L > 4$	0.37 ± 0.07	21.5 ± 5.7

This interpretation has however serious difficulties, especially in the case of the parameter β. First, the pion source is most unlikely to be spherical in the event rest frame. The effective size of the source in the pion pair rest frame is dependent on both the space and time structure in the event rest frame and is dependent on the Lorentz transformation between the event and the pair rest frame. Secondly, if the true distribution in Q^2 is not Gaussian, but possesses an unobserved spike at very low Q^2 coming from large scale structure, the interpretation of α in terms of incoherence fails.

6. Conclusions

We have studied the correlations between the charged particles produced in e^+e^- annihilations $e^+e^- \rightarrow$ hadrons in the c.m. energy interval 29 to 37 GeV.

The multiplicities in opposite jets are very weakly correlated. The observed weak correlation has two trivial sources: our experimental multiplicity cut and the presence of heavy quarks in e^+e^- annihilations. This is in contrast to the observations made for pp and $p\bar{p}$ interactions for which these correlations were found to be stronger.

We observe strong two particle rapidity correlations of the range of about one unit in rapidity. The contribution of the resonance decays to these correlations depends on rapidity: it is small for small rapidities ($|y| < 1$), and becomes dominating for large rapidities.

Our study confirmed the existence of two particle charge correlations of short range in rapidity. These short range ($|y - y_t| \leq 1$) correlations, observed in all rapidity regions demonstrate that the particle charges are compensated locally, and they are mainly due to the short range order in the fragmentation

process. The data are in agreement with the Lund model MC calculation, which has long range charge correlations built in.

We observe correlation effects due to Bose-Einstein statistics, the so called GGLP effect, in both two and three particle combinations.

References

1. TASSO Collab. R. Brandelik et al.: Phys. Lett. **100 B**, 357 (1981)
2. W. Koch, Proc. of the International Symposium on Multiparticle Dynamics, p. 534. Volendam (1982)
3. G. Giacomelli, M. Jacob: Phys. Rep. **55**, 1 (1979); J. Whitmore: Phys. Rep. **27 C**, 187 (1976)
4. G. Goldhaber: The GGLP effect from 1959 to 1984. LBL-19417 (1985)
5. TASSO Collab. M. Althoff et al.: Z. Phys. C – Particles and Fields **22**, 307 (1984)
6. R.D. Field, R.P. Feynman: Nucl. Phys. **B 136**, 1 (1978); P. Hoyer et al.: Nucl. Phys. **B 161**, 349 (1979)
7. B. Andersson, G. Gustafson, T. Sjostrand: Phys. Lett. **94 B**, 211 (1980) (version 4.3)
8. TASSO Collab. R. Brandelik et al.: Phys. Lett. **94 B**, 437 (1980)
9. C. Peterson et al.: Phys. Rev. **D 27**, 105 (1983)
10. S. Uhlig et al.: Nucl. Phys. **B 132**, 15 (1978)
11. UA5 Collab. K. Alpgard et al.: Phys. Lett. **123 B**, 361 (1983)
12. K. Fialkowski, A. Kotanski: Phys. Lett. **115 B**, 425 (1982); A. Capella, J. Tran Thanh Van: Z. Phys. C – Particles and Fields **18**, 85 (1983); A. Capella, A. Krzywicki: Phys. Rev. **D 18**, 4120 (1978)
13. Pisa-Stony Brook Collab. S.R. Amendolia et al.: Phys. Lett. **50 B**, 396 (1974); Nuovo Cimento **31 A**, 17 (1976)
14. R. Slansky: Phys. Rep. **11 C**, 99 (1974); L. Foa: Phys. Rep. **22 C**, 1 (1975)
15. A. Breakstone et al.: Phys. Lett. **114 B**, 383 (1982)
16. A. Capella: Proc. Europhysics Study Conference, p. 199. Erice (1981)
17. PLUTO Collab. Ch. Berger et al.: Nucl. Phys. **B 214**, 189 (1983)
18. TPC Collab. H. Aihara et al.: Phys. Rev. Lett. **53**, 2199 (1984)
19. G. Goldhaber, S. Goldhaber, W. Lee, A. Pais: Phys. Rev. **120**, 300 (1960)
20. G. Cocconi: Phys. Lett. **49 B**, 459 (1974); E.V. Shuryak: Phys. Lett. **44 B**, 387 (1973)
21. G.I. Kopylov, M.I. Podgoretski: Sov. J. Nucl. Phys. **15**, 219 (1972)
22. M. Gyulassy, S.M. Kauffmann, L.W. Wilson: Phys. Rev. **C 20**, 2267 (1979)
23. G. Goldhaber: Multipion Correlations in e^+e^- Annihilation at SPEAR. Presented at the International Conference on High Energy Physics, Lisbon 1981; report LBL-13291
24. TPC Collab. H. Aihara et al.: Phys. Rev. **D 31**, 996 (1985)